Relativistic Calculation of the Deuteron Electromagnetic Form Factor. I*

FRANZ GROSS†
Palmer Physical Laboratory, Princeton University, Princeton, New Jersey
(Received 9 December 1963)

The foundations of a relativistic theory of the deuteron-electromagnetic form factor are discussed. The theory is based on single-variable unsubtracted dispersion relations and coupled unitarity equations. Because of the presence of very low anomalous thresholds, only a few diagrams need be considered to give a satisfactory low-momentum transfer theory, and the diagrams with thresholds below $36\mu^2$ are tabulated. The scalar theory for a subset of these diagrams (corresponding to a one-pion-exchange approximation) is examined and found to be in close correspondence with potential theory. Special attention is given to the anomalous thresholds. The role of the 3-pion state is discussed. Numerical calculations are reserved for future papers.

1. INTRODUCTION AND SUMMARY

THE deuteron, as the only bound state of two nucleons, has been a subject of interest to physicists since the discovery of the neutron. However, until the advent of high-energy electron scattering experiments in the last decade, the only experimental data available regarding the deuteron were its binding energy, effective range, and static moments: charge, magnetic moment, and quadrupole moment.[1] As a result, little information could be obtained from the deuteron regarding the detailed nature of the nuclear force.

With the use of high-energy electron scattering experiments, one can now measure the matrix element shown in Fig. 1, which is commonly called the deuteron form factor. Measurements have been made by McIntyre and Burleson,[2] Friedman, Kendall, and Gram,[3] Littauer, Schopper, and Wilson,[4] Friedman and Kendall,[5] Grossetete and Lehmann,[6] Drickey and Hand,[7] and Erikson.[8]

The deuteron form factor depends only on the momentum transfer, $s=q^2$, the physical region being $s<0$. By assuming crossing symmetry, one can obtain the annihilation form factor from the scattering form factor, its physical region corresponding to $s>4M^2$. Both form factors can be expressed in terms of three scalar functions of q^2, G_C, G_M, G_Q, which are the charge, magnetic moment, and quadrupole-moment form factors. The electron scattering experiments mentioned above can only give us information about two combinations of these three invariants $[G_C^2+2(s/6M^2)^2G_Q^2$ and G_M^2 for example$]$ but this can already give us considerable insight into the detailed behavior of nuclear forces. It is the purpose of this paper to lay the foundations for a relativistic calculation of the form factor using the techniques of single-variable dispersion relations and generalized unitarity. In a later paper we will describe a calculation based on these considerations.[9] Jones[10] has done a less extensive calculation along similar lines, and Nuttall[11] has independently obtained many of the results in this paper.

Before we introduce and summarize our work, it is desirable to review briefly the progress on this problem to date.

The literature on this subject is quite extensive, as an examination of Ref. 1 will indicate. It is true, however, that very little success has been achieved in obtaining a fundamental relativistic theory of the deuteron. The

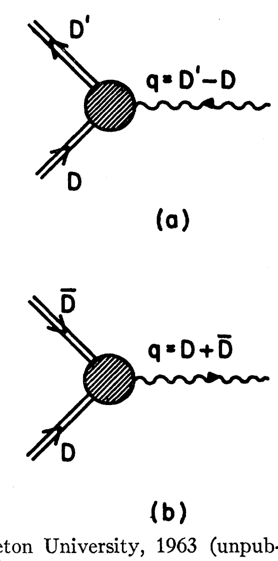

FIG. 1. The deuteron form factor (a) in the scattering channel (physical region $s<0$) and (b) in the annihilation channel (physical region $s>4M^2$).

* This paper is based in part on a thesis submitted to Princeton University in partial fulfillment of the requirements for the Ph.D. degree. Work supported in part by the U. S. Air Force Office of Scientific Research.

† Present address: Laboratory of Nuclear Studies, Cornell University, Ithaca, New York.

[1] L. Hulthén and M. Sugawara, *Handbuch der Physik*, edited by S. Flügge (Springer-Verlag, Berlin, 1957), Vol. XXXIX, p. 69.

[2] J. A. McIntyre and G. R. Burleson, Phys. Rev. **112**, 2077 (1958); **112**, 1155 (1958).

[3] J. I. Friedman, H. W. Kendall, and P. A. M. Gram, Phys. Rev. **120**, 992 (1960).

[4] R. M. Littauer, H. F. Schopper, and R. R. Wilson, Phys. Rev. Letters **7**, 141 (1961).

[5] J. I. Friedman and H. W. Kendall, Phys. Rev. **129**, 2802 (1963).

[6] B. Grossetete and P. Lehmann, Nuovo Cimento **28**, 423 (1963).

[7] D. J. Drickey and L. N. Hand, Phys. Rev. Letters **9**, 521 (1962).

[8] E. Erikson (to be published).

[9] F. Gross, Ph.D. thesis, Princeton University, 1963 (unpublished); F. Gross (to be published).

[10] H. F. Jones, Nuovo Cimento **26**, 790 (1962).

[11] J. Nuttall, Nuovo Cimento **29**, 841 (1963).

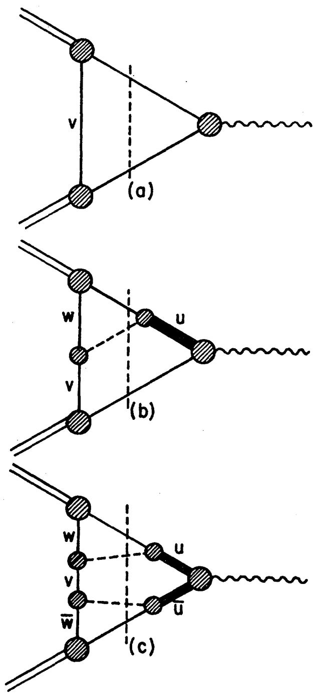

FIG. 2. The three diagrams for which the numerical results have been obtained. Double solid lines represent deuterons or antideuterons, solid lines are nucleons or antinucleons, dotted lines are pions. The vertical dotted line denotes how the diagram is "cut," i.e., which particles are regarded as part of the intermediate state. Heavy solid lines denote nucleons (or antinucleons) which are not on the mass shell. The same key is employed in the following figures as well.

currently popular approach involves choosing a potential for a nonrelativistic Schroedinger equation. The potential is required to behave as the one-pion-exchange approximation (OPE) at large distances (calculated from second-order perturbation theory using a suitable interaction Hamiltonian) and is assumed to have an infinite hard core at a distance of about $(2\mu)^{-1}$. A number of arbitrary parameters are included in the intermediate range, and these are adjusted to fit scattering data and static deuteron data. Two-nucleon potentials have been determined in this way by a number of physicists.[12,13]

After a potential has been chosen, one can use this, and the nonrelativistic theory of Jankus,[14] to analyze the deuteron form factor.[3,6,7,13,15] The Jankus theory leads to an expression for the deuteron form factor in which the isoscalar nucleon form factors appear as a factor:

$$\begin{aligned} G_C(s) &= F_C(s)C_E(s)\,, \\ G_M(s) &= F_C(s)C_L(s)+F_M(s)C_S(s)\,, \qquad (1.1) \\ G_Q(s) &= F_C(s)C_Q(s)\,, \end{aligned}$$

where the C's are known functionals of the deuteron wave function.[16] If one believes this theory, then one can deduce the neutron form factor from deuteron and proton form factor data. Conversely, one could take neutron form factor data obtained from, say, the inelastic experiment and obtain information about the deuteron. At high momentum transfer the latter procedure is probably the least subject to ambiguity.

No matter which point of view one takes, the above approach to the deuteron has several limitations which have already been discussed by Gourdin.[16] The most serious limitation in our mind is not in the restriction to a nonrelativistic wave function, but in the Jankus theory itself. This theory gives no indication of what has been left out, or how to calculate "corrections." These corrections include the effects of exchange currents and off-mass-shell contributions arising from the fact that the nucleons are bound and not free. In principle, the only way even to define these correction terms is to have a theory which is fully relativistic and which, perhaps, can be made to reduce to the Jankus potential theory at low energies. Then one can isolate the correction terms, and try to calculate them. Until one has such a theory, one can do no more than guess at the size of the errors involved, although it is reasonable to believe they are small at low-momentum transfer.

An additional limitation of the potential theories is that they invariably involve a number of undetermined parameters, which are adjusted to fit the data. It would be most gratifying to have a theory which had no such parameters, so that one could claim a fundamental determination of some of the deuteron static moments.

This brings us naturally to the objectives of the present paper. We are interested in developing the foundations of a fully relativistic theory of the deuteron which is fundamental in the sense that very few phenomenological parameters occur, and in the sense that all of the effects which must be taken into account are included. Such a theory could then serve as a basis from which to make approximate calculations.

Let us hasten to add that what we present here represents only a partial step toward realizing the above objectives. However, a calculation has been performed which seems to us to justify this approach,[9] but it is by no means clear at this time that this approach to the deuteron will ultimately prove to be the best. Furthermore, at present our calculations are not sufficiently complete to compete with potential theory as a research tool. Their principal value at the moment seems to be in verifying in detail long-held convictions that the S-matrix theory of scattering processes already contains the description of bound states.

In Sec. 2 of this paper we discuss the diagrams which should be considered in a relativistic calculation and isolate those which have the lowest threshold. We also discuss a particular class of diagrams which seems to relate closely to potential theory. The diagrams in Fig. 2 are the first three members of this class and as such play a central role in any calculation. In Sec. 3, we present the calculation of the diagrams in Fig. 2 for the case where all of the particles are spinless and show how the

[12] S. Gartenhaus, Phys. Rev. **100**, 900 (1955); T. Hamada and I. D. Johnston, Nucl. Phys. **34**, 382 (1962).
[13] N. K. Glendenning and G. Kramer, Phys. Rev. **126**, 3159 (1962).
[14] V. Z. Jankus, Phys. Rev. **102**, 1586 (1956).
[15] J. A. McIntyre and S. Dhar, Phys. Rev. **106**, 1074 (1957).
[16] M. Gourdin, Nuovo Cimento **28**, 533 (1963).

deuteron vertex calculated by Blankenbecler and Cook[17]

$$\Gamma = \langle N | f_p | D \rangle$$

plays a role similar to that played by the deuteron wave function. This complements the work of a number of authors[17–19] and enables us to make a direct comparison between relativistic theory and potential theory. Then, in Sec. 4 we lay more carefully the foundations for a relativistic theory using a modified form of the Blankenbecler[20] matrix N/D method. Our analysis is general enough to include spin and we clarify a number of questions in this section pertaining to the decomposition of the form factor into additive and nonadditive parts.

A full numerical calculation with spin based on the diagrams in Fig. 2 has been carried out.[9] By assuming known values of the pion-nucleon coupling constant, and that unsubtracted dispersion relations are valid, the three deuteron form factors can be calculated in terms of only one free parameter, which can be interpreted nonrelativistically as the normalization constant of the wave function. If this is chosen to give the correct charge, one completely determines the invariant functions, which agree with known experimental data to within 10%.

Throughout the paper we have let M = deuteron mass, m = nucleon mass, and μ = pion mass.

2. SURVEY OF CONTRIBUTING DIAGRAMS

In this section we undertake a systematic study of the diagrams which contribute to the form factor of the deuteron. Although our discussion has the flavor of perturbation theory, it is not based on perturbation theory, but on dispersion relations with unitarity. This means that our diagrams are not Feynman integrals but dispersion integrals, and as such include (1) the particles which are to be regarded as the intermediate state (indicated by a dotted "cut" in the diagram), (2) the approximations to be taken for the initial and final amplitudes when evaluating the absorptive part. Hence, each diagram represents a cut and the corresponding discontinuity across that cut in the complex s plane. All diagrams have cuts along $s>0$ only, and according to the usual assumptions in dispersion theory, those diagrams with the lowest thresholds (thresholds closest to the physical region $s<0$) are regarded as the most important while those with higher thresholds are neglected, or treated phenomenologically. We will limit ourselves to a world of nucleons and pions only.

In the usual situation in which dispersion theory is employed, the use of diagrams is of little more than symbolic value, because the initial and final amplitudes are unknown, and all diagrams involving the same intermediate state have the same threshold. Hence, in this case, dispersion theory provides no justification for choosing one approximation over another. The presence of anomalous thresholds changes the picture however; in this case one approximation for an initial or final amplitude will often have a lower threshold than the others, and hence can be taken as a legitimate first approximation. In the case of the deuteron form factor this situation occurs in the extreme, and there are only a few diagrams (which can be calculated approximately) with the lowest thresholds. It is our intention in this section to display those diagrams with the lowest thresholds.

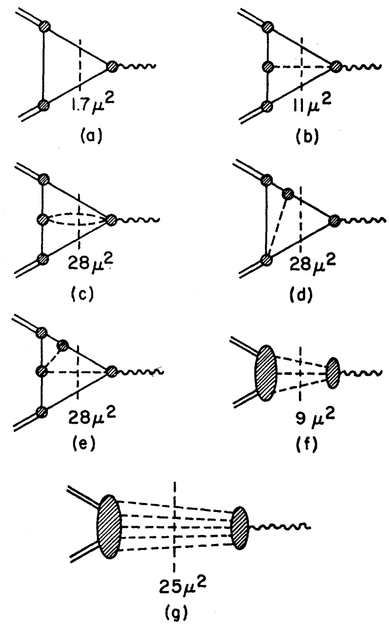

FIG. 3. Complete set of diagrams with thresholds below $36\mu^2$. The thresholds are marked below each diagram. For a key to the diagrams see the caption to Fig. 2.

The famous nucleon triangle diagram has been well discussed elsewhere.[10,19,21] It is known to have the lowest threshold, which is at $1.73\mu^2$. Since the normal threshold for this process is at $4m^2 \cong 181\mu^2$ ($m = 6.72\ \mu$), the significance of the anomalous region is overwhelming. Furthermore, this single diagram provides the *exact* contribution to the imaginary part up to the threshold for the 3-pion state, $9\mu^2$, and it can be calculated. However, one can show that this diagram cannot provide a very good approximation by itself.[9]

There are many diagrams which contribute above $9\mu^2$; to list them all is an impossible task. What we will content ourselves with here is to present a partial list of some of the more interesting diagrams. First, in Fig. 3 we present a complete list of all of those diagrams with thresholds below $36\mu^2$. The choice of $36\mu^2$ is somewhat arbitrary. Above $36\mu^2$, a great many more dia-

[17] R. Blankenbecler and L. F. Cook, Jr., Phys. Rev. **119**, 1745 (1960).

[18] L. Bertocchi, C. Ceolin, and M. Tonin, Nuovo Cimento **18**, 770 (1960).

[19] R. E. Cutkosky, *Proceedings of the 1960 Annual International Conference on High-Energy Physics at Rochester* (Interscience Publishers, Inc., New York, 1960), Vol. 10, p. 236; L. Durand, III, Phys. Rev. **123**, 1393 (1961).

[20] R. Blankenbecler, Phys. Rev. **122**, 533 (1963).

[21] R. Blankenbecler and Y. Nambu, Nuovo Cimento **18**, 595 (1960).

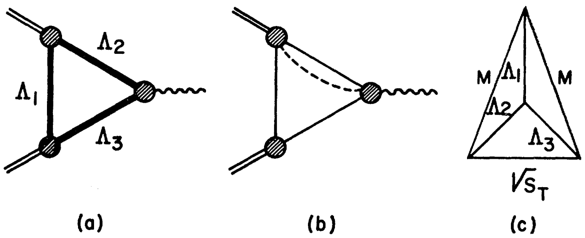

FIG. 4. (a) General diagram used to generate diagrams in Fig. 3. (b) Specific example of diagram shown in (a) with $\Lambda_1=m$, $\Lambda_2=m+\mu$, $\Lambda_3=m$. (c) Dual diagram corresponding to (a).

grams contribute than can be easily discussed, and hence the absorptive part above this threshold will probably have to be estimated in some approximate manner anyway. In addition, one can show roughly that contributions to the absorptive part above a given energy s do not become important until a distance of approximately a $\sim 4/s^{1/2}$. For $s^{1/2}=6\,\mu$, the relevant radius is 0.67 pion Compton wavelengths or about 1 F. Hence, the precise structure of diagrams with thresholds above $36\mu^2$ should not matter, and it can be hoped that a careful treatment below $36\mu^2$ coupled with some reasonable estimates for the absorptive part above this region would give a good relativistic description of the low-energy properties of the deuteron.

In our future discussion we shall ignore the 3- and 5-pion intermediate states, the diagrams shown in Fig. 3(f) and 3(g). It is our feeling that the contribution of these diagrams is not negligible but a serious attempt to estimate their magnitude is difficult and is planned for a later paper. We will have more to say about these diagrams in Sec. 4.

It is perhaps worthwhile to sketch in detail how the rest of the diagrams in Fig. 3 were chosen. We begin by considering the general class of diagrams shown in Fig. 4(a). An example is shown in Fig. 4(b). The masses Λ_1, Λ_2, and Λ_3 are the combined masses of nucleons and pions exchanged across each leg of the fundamental triangle. Now it can be shown that the threshold for such a dispersion integral is the same as the threshold for the corresponding Feynman integral, where the Λ_i are regarded as discrete masses. But this threshold can be easily calculated using the technique of dual diagrams.[22] [The dual of Fig. 4(a) is shown in Fig. 4(c).] One obtains easily

$$s_T=\frac{1}{4\Lambda_1^2}[\Delta(\Lambda_1,\Lambda_2)+\Delta(\Lambda_1,\Lambda_3)]^2-\frac{(\Lambda_2^2-\Lambda_3^2)^2}{4\Lambda_1^2}, \quad (2.1)$$

where,

$$\Delta(a,b)=\Delta(b,a)=\{[a^2-(M-b)^2][(M+b)^2-a^2]\}^{1/2}.$$

If we write

$$\Lambda_i^2=m^2+2\lambda_i,$$

then to a good approximation for small λ_i

$$s_T(\lambda_1\lambda_2\lambda_3)=4((\alpha^2+\lambda_1+\lambda_2)^{1/2}+(\alpha^2+\lambda_1+\lambda_3)^{1/2})^2, \quad (2.2)$$

where $\alpha^2=m\epsilon$ and ϵ is the deuteron binding energy. Hence, the threshold is monotonic in the masses, and increases rapidly with the differences $\Lambda_i^2-m^2$.

Now since the particles in the intermediate state must always be on the mass shell in dispersion theory, the only values of λ which need be considered correspond to those values for which this is possible. If $\Lambda=m+\mu$, then $\lambda\cong 7.22\mu^2$, and the thresholds are all above $36\mu^2$. Hence, the only cases which need be considered are those for which the deuteron vertex has an anomalous threshold. All such cases have been shown in Fig. 3, and their corresponding thresholds as calculated from Eq. (2.2) have been so indicated. In the next section we shall see in detail how this happens in a few special cases, and hence we shall not discuss it further here.

The diagrams presented in Fig. 3 cannot be calculated easily, because they contain unknown form factors. To simplify the calculation we can express these form factors in terms of the nucleon form factor by introducing the pole approximation. For example, denoting the nucleon-antinucleon pion form factor shown in Fig. 3(b) by F_4, we have for spinless particles

$$F_4(s,u\bar{u})=\frac{F_2(s)g}{m^2-u}+\frac{F_2(s)g}{m^2-\bar{u}}+F_4'(s,u\bar{u}), \quad (2.3)$$

where $u^{1/2}$ is the rest mass of the nucleon and pion and $\bar{u}^{1/2}$ the rest mass of the antinucleon and pion, and g is the pion-nucleon coupling constant, F_2 the isoscalar-

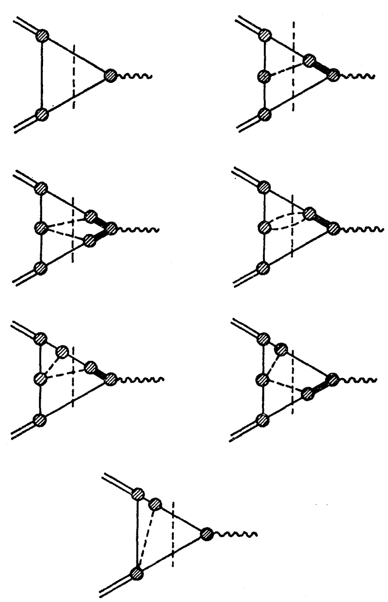

FIG. 5. Diagrams resulting from Fig. 3 when photon form factors are replaced by a pole approximation. The 3- and 5-pion states have been excluded.

[22] See, for example: J. C. Polkinghorne in *1961 Brandeis Summer Institute Lectures in Theoretical Physics* (W. A. Benjamin, Inc., New York, 1962), pp. 118, 130.

nucleon form factor and F_4' the part of the form factor which does not contain a pole in u or $\bar{u}$ at m^2. Retaining only the pole terms of the above expansion (and similarly for F_5, the nucleon-antinucleon 2-pion form factor) one obtains the new set of diagrams shown in Fig. 5. Such an approximation is equivalent to retaining only "additive" terms (a term introduced by Cutkosky[19]), and it appears that the so-called nonadditive terms contain F_4' and F_5' as well as the 3- and 5-pion contribution. Hence, even though it might be difficult to calculate these correction terms in practice, in principle they are clearly delineated, and there is no ambiguity as there would have been had we started from potential theory.

As we have remarked already, we will devote our principal attention to a small but important subclass of the diagrams shown in Fig. 5, and these have already been shown in Fig. 2. The first two diagrams (a) and (b) are those with the lowest threshold, but the choice of the third (c) is less easy to justify. In fact we can present no rigorous justification for its choice, except to say that it (along with the other two) admits a very beautiful interpretation in terms of potential theory. One can, in fact, single out a whole set of such diagrams which admit of an easy interpretation through potential theory. The simplest of these are shown in Fig. 6. We are tempted to call these potential-theory diagrams, with the implication that it is this subclass of diagrams which is described by (Jankus) potential theory. It is not clear that this is a meaningful distinction, or that it is correct. If it is, then one could regard the diagrams in Fig. 5 which are not contained in Fig. 6 as "corrections" to the *additive* part of the form factor. We shall have more to say about this in the next section, but for the moment the detailed relationship between this theory and potential theory awaits further clarification.

3. SCALAR THEORY OF THE DEUTERON

In this section we limit ourselves to scalar particles for pedagogical reasons. Our main goal is to display the structure of the contributions from the three diagrams shown in Fig. 2, with particular emphasis on careful treatment of the anomalous thresholds, and this does not depend on the presence of spin.

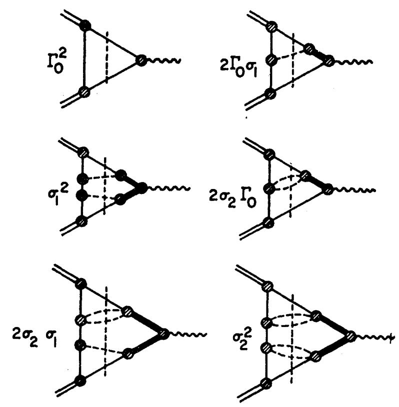

FIG. 6. The first few members of a set of diagrams possessing an immediate interpretation in potential theory. Each diagram contributes a term in the expansion of $(\Gamma_0+\sigma_1+\sigma_2+\cdots)^2$, and these terms are indicated in the figure.

Our results can also be obtained with the use of the Cutkosky rules for obtaining discontinuities of Feynman diagrams.[23] We have not used these rules, however, as they apply to Feynman diagrams and we wish our treatment to apply to the more general dispersion theory diagrams. While it may be true that the two approaches are equivalent in these simple cases discussed here, we feel that confusion can be avoided by doing the continuations explicitly.

It is necessary to adopt a notation and develop the kinematics of 2-, 3-, and 4-particle intermediate states. Our choice of variables is illustrated in Fig. 7. For two particles we choose $s=(n_1+n_2)^2$ and the angle Ω between n_1 and a reference axis in the center-of-mass system. For three particles we choose *either* $s=(n_1+n_2+n_3)^2$, $u=(n_1+n_2)^2$, Σ—the orientation of the 1–2 pair with respect to an arbitrary axis in the center of mass of the 1–2 pair, and Ω—the angle between n_3 and a reference axis in the total center of mass; *or* s, u', Σ', Ω', the same set of variables with n_1 and n_3 interchanged. For four particles we choose $s=(n_1+n_2+n_3+n_4)^2$, $u_1=(n_1+n_3)^2$, $u_2=(n_2+n_4)^2$, Σ_1—the orientation of the 1–3 pair with respect to an arbitrary axis in the center of mass of the 1–3 pair, Σ_2—the orientation of the 2–4 pair in its center of mass and Ω—the orientation of n_1+n_3 in the over-all center of mass.

With this choice of variables, the 2-, 3-, and 4-particle phase space integrals can be reduced to a convenient form.

$$\int \frac{d^3\mathbf{n}_1 d^3\mathbf{n}_2}{(2\pi)^3 4n_1^0 n_2^0}\delta^4(n_1+n_2-s^{1/2})=\int \rho(s;mm)d\Omega\,,$$

$$\int \frac{d^3\mathbf{n}_1 d^3\mathbf{n}_2 d^3\mathbf{k}}{(2\pi)^6 8n_1^0 n_2^0 k^0}\delta^4(n_1+n_2+k-s^{1/2})=\int \rho(s;u^{1/2}m)\rho(u;m\mu)d\Omega du d\Sigma\,, \tag{3.1}$$

$$\int \frac{d^3\mathbf{n}_1 d^3\mathbf{n}_2 d^3\mathbf{k}_1 d^3\mathbf{k}_2}{(2\pi)^9 16n_1^0 n_2^0 k_1^0 k_2^0}\delta^4(n_1+n_2+k_1+k_2-s^{1/2})=\int \rho(s;u_1^{1/2}u_2^{1/2})\rho(u_1;m\mu)\rho(u_2;m\mu)d\Omega du_1 du_2 d\Sigma_1 d\Sigma_2\,,$$

[23] R. E. Cutkosky, J. Math. Phys. 1, 429 (1960).

where the n_i are nucleon four momenta and the k_i meson four-momenta and

$$n_i^2=m^2,\quad k_i^2=\mu^2,$$

$$\rho(s;m_1m_2)=\frac{1}{(2\pi)^3}\frac{Q(s;m_1m_2)}{4s^{1/2}}\theta[s-(m_1+m_2)^2],$$

$$Q(s;m_1m_2)=\left(\frac{[s-(m_1+m_2)^2][s-(m_1-m_2)^2]}{4s}\right)^{1/2}. \tag{3.2}$$

Let us now turn to an examination of the integrals corresponding to the diagrams in Fig. 2. If the isotopic nucleon form factor is denoted by $F(s)$, the deuteron-nucleon coupling constant by Γ_0, and the pion-nucleon coupling constant by g, then the deuteron form factor, $G(s)$, becomes (for small M^2)

$$G(s)=\frac{1}{\pi}\int_{s_0}^{\infty}\frac{\mathrm{Im}G(s')}{s'-s}ds',$$

$$\mathrm{Im}G(s)=(2\pi)\pi\int_{-1}^{+1}dz_v\rho(s;mm)\frac{\Gamma_0^2F(s)}{m^2-v}+(2\pi)^3\int_{(m+\mu)^2}^{\infty}du\int_{-1}^{+1}dz_vdz_w\frac{\rho(s;mu^{1/2})\rho(u;m\mu)\Gamma_0^2g^2F(s)}{(m^2-u)(m^2-v)(m^2-w)}$$
$$+(2\pi)^3\pi\int_{(m+\mu)^2}^{\infty}du\int_{(m+\mu)^2}^{\infty}d\bar{u}\int_{-1}^{+1}dz_vdz_wdz_{\bar{w}}\frac{\rho(s;u^{1/2}\bar{u}^{1/2})\rho(u;m\mu)\rho(\bar{u};m\mu)\Gamma_0^2g^4F(s)}{(m^2-u)(m^2-\bar{u})(m^2-v)(m^2-w)(m^2-\bar{w})}. \tag{3.3}$$

We have performed the ϕ integrations. Note also the extra factor of 2 in the second term, because there are two such diagrams which contribute to this term. The variable z_v is the cosine of the angle on which v depends, and the angles are defined so that this integration is always in the rest system of the virtual particle which corresponds to v. For definitions of u, $\bar{u}$, v, w, and $\bar{w}$ see Fig. 2.

Equation (3.3) is obtained by the application of unitarity to the diagrams in Fig. 2. In applying the unitarity argument we assume that M is very small, so that the thresholds of the various intermediate states will be greater than the physical threshold at $4M^2$. Then, we will give M^2 a small imaginary part (its sign does not matter) and continue M^2 to physical values.[21,24] This will give rise to the anomalous thresholds, and a resulting simplification of the above equation.

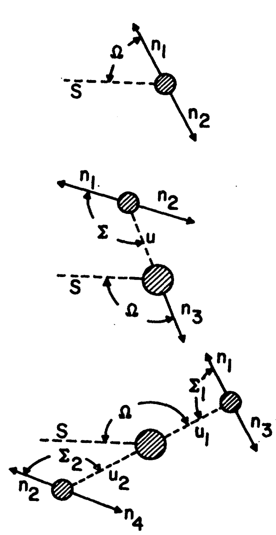

FIG. 7. Representation of choice of variables used to describe 2-, 3-, and 4-particle intermediate states.

Before we proceed with the calculation we wish to call attention to the curious fact that Eq. (3.3) as it stands

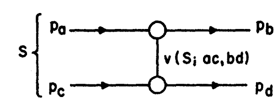

FIG. 8. Pole diagram illustrating the definition of $v(s;ac,bd)$.

is certainly a bad approximation to the absorptive part of the deuteron form factor. Above $9\mu^2$, $F(s)$ is complex, but the rest of the equation is real, and hence, if we took Eq. (3.3) literally, $\mathrm{Im}G$ would be complex and G would not be a real analytic function. This is certainly wrong for, among other things, it would imply that the charge, magnetic moment, and quadrupole moments were complex! The resolution to this difficulty lies in the fact that we have neglected the very important contribution of the three-pion intermediate state, which if included would presumably cancel the imaginary part of (3.3) making the total expression real. Hence, to be consistent, we must regard $F(s)$ as real in Eq. (3.3). Such a drastic approximation is by no means a limitation on the present calculation, however, for the situation can be handled very nicely (and correctly) by treating the problem as a coupled-channel problem. Such a formulation is sketched in the next section, and for the time being we will regard F as real, waiting for the next section to make things right. Let us return now to the calculation.

[24] S. Mandelstam, Phys. Rev. Letters 4, 84 (1960).

Next we express v, w, and $\bar{w}$ in terms of z_v, z_w and $z_{\bar{w}}$. We note that the magnitude of the relative three-momentum of two particles of masses a and b and total energy s in their center-of-mass system is

$$Q(s;ab)=\left(\frac{[s-(a+b)^2][s-(a-b)^2]}{4s}\right)^{1/2}. \quad (3.4)$$

This is the same Q that occurred in Eq. (3.2). Note that the total energy of the particle of mass a is

$$Q_0(s;ab)=[a^2+Q^2(s;ab)]^{1/2}$$
$$=\frac{1}{2s^{1/2}}(s+a^2-b^2). \quad (3.5)$$

In general, a v will have the form

$$v=(p_a-p_b)^2=a^2+b^2=2Q_0(s;ac)Q_0(s;bd)$$
$$+2Q(s;ac)Q(s;bd)z_v,$$

where the masses of the particles involved are a, b, c, and d and $s=(p_a+p_c)^2$ (see Fig. 8). Hence, we introduce the general notation: $v=v(s;ac,bd)$. Further, if we define the integral

$$\mu(u,v)=\frac{2\pi}{m^2-u}\int_{-1}^{+1}dz_w\frac{g^2\Gamma_0\rho(u;m\mu)}{m^2-w(u;m\mu,Mv)}, \quad (3.6)$$

then we can write Eq. (3.3) as

$$\mathrm{Im}G(s)=2\pi^2F(s)\left\{\rho(s;mm)\int_{-1}^{+1}dz_v\frac{\Gamma_0^2}{m^2-v(s;mm,MM)}+2\int_{(m+\mu)^2}^{\infty}du\rho(s;u^{1/2}m)\int_{-1}^{+1}dz_v\frac{\mu(u,v)}{m^2-v(s;mu^{1/2},MM)}\right.$$
$$\left.+\int_{(m+\mu)^2}^{\infty}du\int_{(m+\mu)^2}^{\infty}d\bar{u}\rho(s;u^{1/2}\bar{u}^{1/2})\int_{-1}^{+1}dz_v\frac{\mu(u,v)\mu(\bar{u},v)}{m^2-v(s;u^{1/2}\bar{u}^{1/2},MM)}\right\}. \quad (3.7)$$

These equations are valid for small M. Making use of the corollary in the Appendix we cast (3.7) into a form more suitable for continuation in M^2:

$$\mathrm{Im}G(s)=2\pi^2F(s)\left\{\rho(s;mm)\int_{-\infty}^{a_2}\frac{\Gamma_0^2ds'}{2Q(s';mm)Q(s';MM)(s'-s)}\right.$$
$$+2\int_{(m+\mu)^2}^{\infty}du\rho(s,mu^{1/2})\mu(u,m^2)\int_{-\infty}^{a_4}\frac{\Gamma_0ds'}{2Q(s';mu^{1/2})Q(s';MM)(s'-s)}$$
$$\left.+\int_{(m+\mu)^2}^{\infty}du\int_{(m+\mu)^2}^{\infty}d\bar{u}\rho(s;u^{1/2}\bar{u}^{1/2})\mu(u,m^2)\mu(\bar{u},m^2)\int_{-\infty}^{a_5}\frac{ds'}{2Q(s';u^{1/2}\bar{u}^{1/2})Q(s';MM)(s'-s)}\right\}, \quad (3.8)$$

where a_2, a_4, and a_5 are functions of M and u and can be calculated as described in the Appendix. We have defined $z^{1/2}=|z|^{1/2}e^{(i\arg z)/2}$.

We interrupt our argument at this point to consider the deuteron-nucleon vertex (shown in Fig. 9). The imaginary part of this vertex (OPE approximation) is, for small M

$$\mathrm{Im}\Gamma(u)=2\pi^2\rho(u;m\mu)\int_{-1}^{+1}dz_v\frac{g^2\Gamma_0}{m^2-v(u;m\mu,Mm)}. \quad (3.9)$$

But note that

$$\mu(u,m^2)=\mathrm{Im}\Gamma(u)/\pi(m^2-u). \quad (3.10)$$

Hence, it is clear that the deuteron-nucleon vertex plays a central role in the calculation.

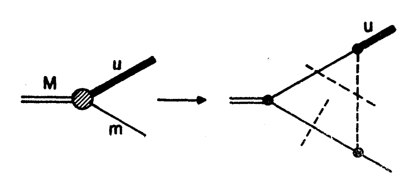

FIG. 9. The deuteron nucleon vertex, in the one-pion exchange approximation.

Let us continue M^2 to obtain the physical deuteron-nucleon vertex. For $M^2\approx m^2$, we have

$$\Gamma(u)=\frac{1}{\pi}\int_{(m+\mu)^2}^{\infty}\frac{2\pi^2\rho(u;m\mu)}{u'-u}du'\left(\int_{a_-}^{a_+}+\int_{-\infty}^{0}\right)$$
$$\times\frac{du''g^2\Gamma_0}{2Q(u'';m\mu)Q(u'';Mm)(u''-u')}, \quad (3.11)$$

where a_+ and a_- as a function of M^2 are

$$a_\pm=m^2+\frac{M^2\mu^2}{2m^2}\pm2M\mu\left(1-\frac{M^2}{4m^2}\right)^{1/2}\left(1-\frac{\mu^2}{4m^2}\right)^{1/2}, \quad (3.12)$$

and the correct signs have been determined by examination of $\mathrm{sgn}(p'(s))$ as in the Appendix. Now give M^2 a small (negative) imaginary part and do the continuation. As M^2 increases, a_+ increases, until at $M^2\approx2m^2$, $a_+=(m+\mu)^2$, and for larger M^2, a_+ decreases. A careful examination shows that in fact a_+ passes above $(m+\mu)^2$, so that the contour must be deformed. Hence, we obtain

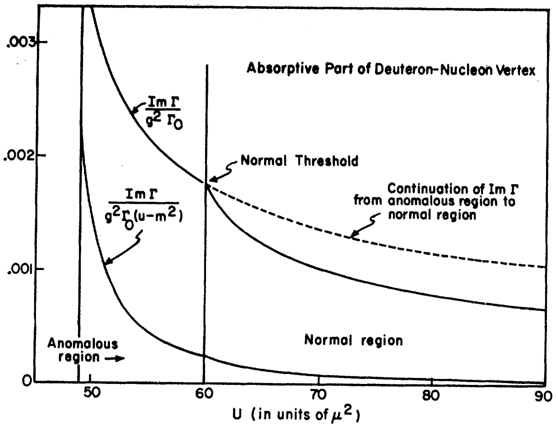

FIG. 10. Absorptive part of the deuteron-nucleon vertex in the normal and anomalous region.

from the Appendix

$$\Gamma(u)=\frac{1}{\pi}\int_{u_0}^{(m+\mu)^2}\frac{(-2\pi i)(2\pi)^2\rho(u';m\mu)g^2\Gamma_0}{2Q(u';m\mu)Q(u',Mm)(u'-u)}du'+\frac{1}{\pi}\int_{(m+\mu)^2}^{\infty}\frac{B(u')}{u'-u}du', \quad (3.13)$$

where $B(u)$ can be calculated using the Appendix, and $u_0=a_+(M^2)\approx m^2+2\mu(\mu+2\alpha)$ (where M^2 is now the physical deuteron mass). Finally, recalling the expression for ρ [Eq. (3.2)], and continuing the integrand, we have

$$\Gamma(u)=\frac{1}{\pi}\int_{u_0}^{(m+\mu)^2}\frac{\mathrm{Im}_A\Gamma(u')}{u'-u}du'+\frac{1}{\pi}\int_{(m+\mu)^2}^{\infty}\frac{B(u')}{u'-u}du', \quad (3.14)$$

where

$$\mathrm{Im}_A\Gamma(u)=\frac{g^2\Gamma_0\theta(u-u_0)\theta[(m+\mu)^2-u]}{8[((M+m)^2-u)(u-(M-m)^2)]^{1/2}}. \quad (3.15)$$

At this time we also obtain $B(u')$. This we can do more easily another way. Going back to Eq. (3.9), we obtain directly

$$\mathrm{Im}\Gamma(u)=\frac{g^2\Gamma_0\theta(u-u_0)}{16\pi\{[u-(M+m)^2][u-(M-m)^2]\}^{1/2}}\times\ln\left(\frac{f(u)+[g'(u)]^{1/2}}{f(u)-[g'(u)]^{1/2}}\right), \quad (3.16)$$

where

$$f(u)=-M^2+\frac{(u+M^2-m^2)}{2u}(u+m^2-\mu^2),$$

$$g'(u)=\frac{1}{4u^2}[u-(M+m)^2][u-(M-m)^2]\times[u-(m+\mu)^2][u-(m-\mu)^2].$$

Since g' is negative for $u<(M+m)^2$ this form of the results is inconvenient, and defining

$$\ln z=\ln|z|+i\arg z,$$

we obtain the following expression valid for $(m+\mu)^2<u<\sim 2m^2$:

$$\mathrm{Im}\Gamma(u)=\frac{g^2\Gamma_0}{8\{[(M+m)^2-u][u-(M-m)^2]\}^{1/2}}\times\left(1+\frac{1}{2\pi}\tan^{-1}\frac{2|g'|^{1/2}f}{f^2-g'}\right). \quad (3.17)$$

Hence, for $u>(m+\mu)^2$ this is B. For $u<(m+\mu)^2$ the discontinuity of (3.16) would again give $\mathrm{Im}_A\Gamma$. For a complete discussion of this, see the article by Blankenbecler and Cook.[17] Note, however, that their dispersion integrals are defined with a $u'-u+i\epsilon$ instead of a $u'-u-i\epsilon$, which introduces an additional minus sign into the definition of the imaginary part.

In Fig. 10 we have plotted ImΓ. The graph shows that ImΓ is quite large near the onset of the anomalous threshold, and falls off to zero as u is increased. Special attention is called to its behavior in the normal region, where it begins to decrease to zero more rapidly. The graph of $(\mathrm{Im}\Gamma/u-m^2)$ possesses this property to an even greater degree. One can see that the neglect of ImΓ in the normal region is not likely to introduce a large error, and this is an approximation we shall make in what follows.

Let us return now to Eq. (3.8), and perform the analytic continuation in M^2. We shall do this in two stages—first we shall continue the M^2 in the u integrals, then we shall continue the M^2 in the s' integral. As indicated above, we shall only retain the anomalous part of the deuteron vertex.

Since the u integrals have precisely the same form as (3.11), we obtain by a direct application of the above arguments

$$\mathrm{Im}G(s)=2\pi^2F(s)\Bigg\{\rho(s;mm)\Gamma_0^2\int_{-\infty}^{a_2}\frac{ds'}{2Q(s';mm)Q(s';MM)(s'-s)}+2\int_{u_0}^{(m+\mu)^2}du\frac{\mathrm{Im}_A\Gamma(u)}{\pi(m^2-u)}\rho(s;mu^{1/2})\Gamma_0\int_{-\infty}^{a_4}\frac{ds'}{2Q(s';mu^{1/2})Q(s';MM)(s'-s)}+\int_{u_0}^{(m+\mu)^2}du\frac{\mathrm{Im}_A\Gamma(u)}{\pi(m^2-u)}\int_{u_0}^{(m+\mu)^2}d\bar{u}\frac{\mathrm{Im}_A\Gamma(\bar{u})}{\pi(m^2-\bar{u})}\rho(s;u^{1/2}\bar{u}^{1/2})\int_{-\infty}^{a_5}\frac{ds'}{2Q(s';u^{1/2}\bar{u}^{1/2})Q(s';MM)(s'-s)}\Bigg\}. \quad (3.18)$$

It remains only to continue the s' integral. To this end we form

$$G(s)=\frac{1}{\pi}\int_{4m^2}^{\infty}\frac{\mathrm{Im}G(s')}{s'-s}ds' \tag{3.19}$$

and do the continuation as in the Appendix. We encounter integrals of the form

$$\begin{aligned}J(s)&=\int_{(b+c)^2}^{\infty}\frac{\rho(s';bc)}{s'-s}ds'\int_{-\infty}^{a(b,c,M^2)}\frac{ds''}{2Q(s'';bc)Q(s'';MM)(s''-s')}\\&=\int_a^{(c+b)^2}\frac{-2\pi i ds'}{s'-s}\frac{\rho(s';bc)}{2Q_c(s';bc)Q_c(s';MM)}+\text{integral above normal threshold},\end{aligned} \tag{3.20}$$

where Q_c is the continuation of Q below the normal threshold. The upper integral is neglected. Observing that

$$\frac{\rho(s';bc)}{2Q_c(s';bc)Q_c(s';MM)}=\frac{i}{(2\pi)^3 4[s'(4M^2-s')]^{1/2}}$$

we finally obtain:

$$J(s)=\frac{1}{\pi}\int_a^{(b+c)^2}\frac{\mathrm{Im}_AJ(s')ds'}{s'-s}, \tag{3.21}$$

where

$$\mathrm{Im}_AJ(s)=\frac{1}{(2\pi)^2 4[s(4M^2-s)]^{1/2}}.$$

Using the above argument, (3.18) becomes in the anomalous region

$$\begin{aligned}\mathrm{Im}_AG(s)=\frac{F(s)}{8[s(4M^2-s)]^{1/2}}\Big\{&\Gamma_0{}^2\theta[s-s_0(m^2,m^2)]-2\int_{u_0}^{(m+\mu)^2}du\mu_A(u)\Gamma_0\theta[s-s_0(m^2,u)]\\&+\int_{u_0}^{(m+\mu)^2}du\int_{u_0}^{(m+\mu)^2}d\bar{u}\mu_A(u)\mu_A(\bar{u})\theta[s-s_0(u,\bar{u})]\Big\},\end{aligned} \tag{3.22}$$

where we have introduced

$$\mu_A(u)=-\frac{\mathrm{Im}_A\Gamma(u)}{\pi(m^2-u)} \tag{3.23}$$

and

$$\begin{aligned}s_0(a^2,b^2)&\cong s_T(0,\tfrac{1}{2}(a^2-m^2),\tfrac{1}{2}(b^2-m^2))\\&=4([\alpha^2+\tfrac{1}{2}(a^2-m^2)]^{1/2}+[\alpha^2+\tfrac{1}{2}(b^2-m^2)]^{1/2})^2.\end{aligned}$$

s_0 is the anomalous threshold for a diagram corresponding to Fig. 4(a), where the two nucleons which annihilate to produce a photon have masses a and b and the exchanged nucleon has mass m. Now, in the case at hand we can see that

$$\begin{aligned}s_0(m^2,m^2)&=16\alpha^2,\\s_0(m^2,m^2+2\eta-2\alpha^2)&=4(\alpha+\eta^{1/2})^2,\\s_0(m^2+2\eta-2\alpha^2,m^2+2\bar{\eta}-2\alpha^2)&=4(\eta^{1/2}+\bar{\eta}^{1/2})^2.\end{aligned} \tag{3.24}$$

Now α is

$$\alpha=(m\epsilon)^{1/2}=0.328\mu,\quad \alpha^2=0.108\mu^2$$

and the smallest value of η, η_0, is determined from u_0.

$$u_0=m^2+2\eta_0-2\alpha^2=m^2+3.32\mu^2,\quad \eta_0\cong1.77\mu^2.$$

Thus, the thresholds for the last two diagrams are just those given in Fig. 2:

$$\begin{aligned}s_{N\bar{N}\pi}&=s_0(m^2,u_0)=4(0.328+1.33)^2\cong11\mu^2,\\s_{N\bar{N}2\pi}&=s_0(u_0,u_0)=4(2.66)^2\cong28\mu^2.\end{aligned} \tag{3.25}$$

Introducing η and $\bar{\eta}$ as variables allows us to write finally a very compact result.

$$G(s)=\frac{F(s)}{\pi}\int_{16\alpha^2}\frac{\mathrm{Im}_A G'(s')ds'}{s'-s}, \tag{3.26a}$$

$$\mathrm{Im}_A G'(s)=\frac{1}{8[s(4M^2-s)]^{1/2}}\bigg\{\Gamma_0^2\theta(s-16\alpha^2)-2\Gamma_0\int_{\eta_0}^{(\frac{1}{2}s^{1/2}-\alpha)^2}d\eta\sigma_A(\eta)\theta(s-11\mu^2)$$
$$+\int_{\eta_0}^{(\frac{1}{2}s^{1/2}-\eta_0{}^{1/2})^2}d\eta\int_{\eta_0}^{(\frac{1}{2}s^{1/2}-\eta^{1/2})^2}d\bar{\eta}\sigma_A(\eta)\sigma_A(\bar{\eta})\theta(s-28\mu^2)\bigg\}, \tag{3.26b}$$

$$=\frac{1}{8[s(4M^2-s)]^{1/2}}\int_{\alpha^2}^{\infty}d\eta\int_{\alpha^2}^{\infty}d\bar{\eta}\sigma(\eta)\sigma(\bar{\eta})\theta[s-4(\eta^{1/2}+\bar{\eta}^{1/2})^2], \tag{3.26c}$$

where

$$\sigma(\eta)=\Gamma_0\delta(\eta-\alpha^2)-\sigma_A(\eta)\theta(\eta-\eta_0)\theta(7.22\mu^2-\eta),$$
$$\sigma_A(\eta)=\frac{\mathrm{Im}_A\Gamma(m^2+2\eta-2\alpha^2)}{\pi(\eta-\alpha^2)}. \tag{3.27}$$

Note that in (3.26a) we have pulled the nucleon form factor out from under the dispersion integral. If the argument of the dispersion integral approaches zero fast enough at infinity and if $F(s)$ were an entire function, then the result obtained from (3.26a) would be identical to the result one would obtain by integrating over $F(s)$.

$$G(s)=\frac{1}{\pi}\int_{16\alpha^2}\frac{F(s')\,\mathrm{Im}_A G'(s')}{s'-s}ds'. \tag{3.28}$$

$F(s)$ is not entire, of course, so if one factors out $F(s)$ from under the integral sign, then one introduces an additional term which has a cut starting at $9\mu^2$ and represents the difference between (3.26a) and (3.28). In the next section we shall display this additional term, and there is every reason to believe that this term will cancel most of the intrinsic 3-pion contribution. This would explain how the 3-pion term could be so important in the isoscalar-nucleon form factor, and not as important in the deuteron form factor, a problem which ostensibly, at least, should depend upon the 3-pion state in a way very similar to the nucleon problem.

Let us close these remarks by recalling the results of the potential theory of spinless deuterons.[18] If the potential can be regarded as a superposition of Yukawa wells, then the wave function can be written as

$$u(r)=\int_{\alpha}^{\infty}\rho(\sigma)e^{-\sigma r}d\sigma, \tag{3.29}$$

and the deuteron form factor becomes

$$G(\mathbf{q}^2)=F(\mathbf{q}^2)\int_0^{\infty}u(r)^2 j_0\left(\frac{qr}{2}\right)dr$$
$$=\frac{F(\mathbf{q}^2)}{\pi}\int_{16\alpha^2}^{\infty}\frac{ds'}{\mathbf{q}^2+s'}\bigg\{\frac{\pi}{s'^{1/2}}$$
$$\times\int_{\alpha}^{\infty}\int_{\alpha}^{\infty}dxdy\rho(x)\rho(y)\theta[s'^{1/2}-2(x+y)]\bigg\}. \tag{3.30}$$

If $s\ll 4M^2$, then this expression is identical to (3.26) providing only that we take $(4M^2-s)^{1/2}\cong 2M$ and:

$$s=-\mathbf{q}^2,$$

$$\frac{1}{2}\left(\frac{\pi}{\eta}\right)^{1/2}\rho(\eta^{1/2})=\frac{1}{(16M)^{1/2}}\sigma(\eta).$$

Hence, the weight function for the wave function becomes

$$\rho(x)=\tfrac{1}{2}(1/M\pi)^{1/2}x\sigma(x^2), \tag{3.31}$$

and we have succeeded in defining a relativistic wave function. If we wish this wave function to go to zero at the origin, then we must have

$$\int_{\alpha}^{\infty}\rho(x)dx=0, \tag{3.32}$$

which could be carried over relativistically to the requirement that

$$\int_{\alpha^2}^{\infty}\sigma(\eta)d\eta=0$$
$$=\Gamma_0-\frac{1}{\pi}\int_{\eta_0}^{7.22}\frac{\mathrm{Im}_A\Gamma(m^2+2\mu\eta-2\alpha^2)}{(\eta-\alpha^2)}d\eta. \tag{3.33}$$

The last requirement is equivalent to:

$$\Gamma_0=\frac{1}{\pi}\int_{u_0{}^2}^{(m+\mu)^2}\frac{\mathrm{Im}_A\Gamma(u)}{u-m^2}du. \tag{3.34}$$

And hence the requirement that the wave function go to zero is equivalent to the relativistic requirement that the deuteron-nucleon vertex invariant be given by an unsubtracted dispersion relation. In general, the one-pion approximation cannot be expected to satisfy the above conditions, and hence, the wave functions determined from this analysis will not go to zero at the origin. At the moment we wish only to observe that Eq. (3.33) provides a natural way to allow approximately for the higher mass states without introducing arbitrary parameters. The point is that whatever is added to $\mathrm{Im}_A\Gamma$ to account for higher states can be required to satisfy conditions like (3.33), and hence its effect can be determined within the theory.

Finally, it seems likely that all of the diagrams shown in Fig. 6 can be analyzed in precisely the same way, and can be understood as providing successively higher approximations (more pions being exchanged) to the deuteron wave function. It is likely that these diagrams can be summed by setting up an integral equation for the deuteron vertex, and hence, one would, in effect, duplicate a Bethe-Salpeter approach to the deuteron.[25] Whether such an approach gives the full story is unclear at the moment, because at higher and higher energies, the diagrams in Fig. 6 represent a smaller and smaller subclass of all the contributions which could be considered.

4. THE UNITARITY EQUATIONS

It is our intention in this section to lay a more careful foundation for the treatment of the deuteron form factor with spin. We will clarify the distinction between additive and nonadditive parts, and present a careful discussion of the manner in which the three-pion state enters the calculation. (For the time being we neglect all other multiple pion states.)

Our discussion is based on the introduction of coupled unitarity equations. We could, if we wished, solve these coupled equations using the matrix N/D method of Blankenbecler.[17] A natural way to introduce spin would be to formulate the unitarity equations in terms of helicity amplitudes, in the way that Cook and Lee treated $N-\pi$ scattering.[9,26] In fact, what we will do here is equivalent to proceeding in this manner (we have even stolen the N/D notation) but has slight technical advantages when applied to a form-factor problem.

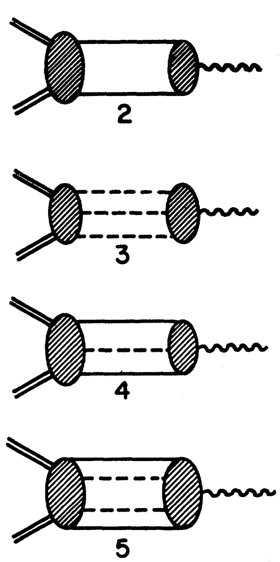

FIG. 11. The four intermediate states (with corresponding channel number beneath) which are retained in the discussion of the deuteron form factor in the text.

[25] J. Tran Thanh Van (to be published).
[26] L. F. Cook, Jr., and B. W. Lee, Phys. Rev. **127**, 283 (1962); **127**, 297 (1962).

We propose, then, to treat the deuteron form factor as part of a coupled system of form factors. The channels we will consider as intermediate states are those shown in Fig. 11. The channels are (numbered from 1 to 5, respectively) the deuteron-antideuteron state (not retained as an intermediate state and hence not shown in Fig. 11), the nucleon-antinucleon state, the three-pion state, the nucleon-antinucleon-pion state, and the nucleon-antinucleon, 2-pion state. Our final equations can be generalized to include the 5-pion state if desired. We shall designate the photon form factor for the nth channel by F_n, and the scattering amplitude from the ith to jth channel by M_{ij}. Then the statement of generalized coupled unitarity is:

$$\mathrm{dis}_s F_i(s,u) = \frac{1}{2i}(F_i(s^+,u)-F_i(s^-,u)) = \sum_j \int du' \rho_j(s,u') F_j(s^+,u'^+) M_{ji}(s^-,u'^-,u)\,, \quad (4.1a)$$

where the integral over u' is meant to represent summation over all of the discrete variables (spins) and integrations over continuous variables (masses of compound systems) of each intermediate state. The s^+ and s^- refer to values of s just above and below the real axis and ρ_j is the phase-space factor (multiplied by π) characteristic of each intermediate state.

We shall immediately adopt a matrix notation, where Eq. (4.1) becomes

$$\mathrm{dis}_s F(s,u) = \int du' F(s^+,u'^+)\rho(s,u') M(s^-,u'^-,u)\,, \quad (4.1b)$$

where ρ is diagonal and F is a row vector. We notice immediately that $\mathrm{dis}_s F(s,u)$ must have no s discontinuity for all $s>s_0$, or else the F will not be a real analytic function (required by time reversal). But this is true only if

$$\int du' F(s^+,u'^+)\rho M(s^-,u'^-,u) = \int du' F(s^-,u'^+)\rho M(s^+,u'^-,u)\,,$$

which leads to the familiar requirement

$$\mathrm{dis}_s M(s,u,u') = \frac{1}{2i}[M(s^+,u,u')-M(s^-,u,u')] = \int du'' M(s^+,u,u''^+)\rho(s,u'') \times M(s^-,u''^-,u')\, s\in R. \quad (4.2)$$

Hence, the scattering matrix M must satisfy coupled unitarity on the right-hand (R) side. This is an important result—it indicates that whatever choice we make for the M's must satisfy coupled unitarity, or else we will obtain a deuteron form factor which is complex in the physical region.

It is clear that if the scattering matrix M is known, we can immediately obtain a solution for the deuteron form factor from (4.1b). Since this form factor has no extra u dependence, we would have

$$\text{dis}_s F_1(s) = \text{Im} F_1(s)\,,$$

and

$$F_1(s) = \frac{1}{\pi}\int \frac{ds'}{s'-s}\,\text{Im} F_1(s')\,. \qquad (4.3)$$

However, Eq. (4.3) is an inconvenient form in which to express the answer, because it necessitates knowing all of the photon form factors F_n in the unphysical region. What we would like instead is an expression of the form (1.1) where the form factors appear factored out of the integral. To this end we can write (in matrix notation)

$$F(s,u) = \int du' F(s,u'^{+})d(s,u'^{-},u) + g(s,u)\,, \qquad (4.4)$$

where g is some entire function of s, and plays the role of a subtraction constant. Let us determine the d matrix in terms of the presumably known scattering amplitudes M.

To begin with, d can have no cuts in the left-hand region, because F has none. In the right-hand region we have

$$\begin{aligned}\text{dis}_s F(s,u) &= \int du' \{\text{dis}_s F(s,u'^{+})d(s^{+},u'^{-},u) \\ &\qquad + F(s^{-},u'^{+})\,\text{dis}_s d(s,u'^{-},u)\} \\ &= \int du' F(s^{-},u'^{+})\rho(s,u')M(s^{+},u'^{-},u)\,, \qquad (4.5)\end{aligned}$$

which gives

$$\begin{aligned}\text{dis}_s d(s,u,u') = \rho(s,u)\int du'' M(s,u,u''^{+}) \\ \times[\delta(u''-u') - d(s,u''^{-},u')]s\in R\,. \qquad (4.6)\end{aligned}$$

This is immediately recognized as the familiar discontinuity of the D function in the N/D method. Our d's are different, however; the relationship is

$$D = 1 - d$$

as one can see by rewriting Eq. (4.4).

One can verify that the unitarity condition (4.2) is sufficient to guarantee that $\text{dis}_s d$ has no cuts on the right-hand Res axis and that therefore Eqs. (4.4) will indeed describe form factors which are real analytic functions. We will therefore assume that the d functions are given by the following integral equations:

$$\begin{aligned}d(s,u,u') = \frac{1}{\pi}\int_R \frac{ds'}{s'-s}\rho(s',u)M(s',u,u') - \frac{1}{\pi}\int_R \frac{ds'}{s'-s} \\ \times\rho(s',u)\int du'' M(s',u,u''^{+})d(s',u''^{-},u')\,. \qquad (4.7)\end{aligned}$$

The remaining problem is to determine the g's. Examination of Eq. (4.7) indicates that $d(s,u,u') \underset{s\to\infty}{\longrightarrow} 0$. Hence, we see that

$$\lim_{s\to-\infty} F(s,u) = g(s,u)\,, \qquad (4.8)$$

and the g's are related to the asymptotic behavior of the form factors. We also see that the g's contain the u dependence of the form factors. In these papers we shall be interested in calculating $F_1(s)$ only, and shall assume that $F_1(s)\to 0$ as $s\to-\infty$. This is a natural assumption in view of the loosely bound nature of the deuteron, and makes unsubtracted dispersion relations valid. Hence, since g is entire we must have $g_1=0$, and this is all we will need to know about the g's.

It should be observed that we have not paid any attention to unitarity in the u variables. Our formalism can be extended to handle this case,[27] but as the deuteron and nucleon form factors have no u dependence, we have decided to neglect this for the time being.

Equations (4.7) have some advantage over the conventional formulation, in that the scattering amplitudes themselves appear in the equations and not their left-hand discontinuities. In treating the 3-pion contribution, this represents a considerable advantage, since if one wishes to assume a phenomenological form for the amplitude (ω and ϕ resonances, for example) this can be directly inserted into the equations without concern for the nature of the left-hand cut. Any set of phenomenological scattering amplitudes can be used, provided only that they satisfy coupled unitarity on the right-hand axis.

One advantage of the above procedure is that we may apply it after the analytic continuation in M^2 has been performed. In this way we can avoid many difficulties which this continuation can introduce into a matrix N/D method.[26]

The inclusion of spin into the above formalism is now seen to be a trivial modification. Once one has the unitarity equations, any appropriate combination of invariants can be chosen to be regarded as the F_i, and one can proceed with the analysis. The relevant M_{ij} are just the factors remaining after the F_i have been factored out. Specifically, either F_1 and F_2, or F_C and F_M can be chosen as the most relevant nucleon form factors. In this work we shall assume F_C and F_M are a

[27] J. S. Ball, W. R. Frazier, and M. Nauenberg, Phys. Rev. **128**, 478 (1962).

more significant combination, because they seem to have a more significant physical interpretation and because they occur naturally if one analyzes the problem using helicity amplitudes.

In practice, our choice of invariants is governed by physical considerations. For example, we will choose the G_C, G_M, and G_Q combinations introduced by Gourdin[16] because it seems natural to assume that unsubtracted dispersion relations exist for these invariants. Also, when we factor out the nucleon form factors we will choose F_C, and not sF_C or F_C/s, for example. This choice depends upon our knowledge of the asymptotic behavior of the amplitudes.[9] Also, the nasty question of kinematical cuts will not trouble us when we pursue the analysis in this fashion.

Let us now specifically discuss the equations for the deuteron form factor. We will take the unitarity equations to be of the following form:

$$\mathrm{Im}G_i(s)=F_C(s)A_i^C(s)+F_M(s)A_i^M(s)+\int duF_3(s,u)M_i^3(s,u)+\int duF_{NA}(s,u)M_i^{NA}(s,u)\,, \quad (4.9)$$

where the A's are the absorptive parts in the anomalous region obtained from graphs of the type shown in Fig. 5, the $F_{NA}M_i^{NA}$ are the remaining contributions which arise from the differences between Fig. 5 and Fig. 3 [as included in Eq. (2.3)] and M^3 is the contribution from the 3π state. (To include the 5π state it is necessary only to interpret F_3 and M_i^3 as matrices.) In addition, we will assume that the nucleon form factor and the 3-pion form factors are dominated by the 3-pion intermediate state.

$$\begin{aligned}
\mathrm{Im}F_C(s)&=\int F_3(s,u)M_C^3(s,u)du\,,\\
\mathrm{Im}F_M(s)&=\int F_3(s,u)M_M^3(s,u)du\,,\\
\mathrm{dis}_sF_3(s,u)&=\int du'F_3(s,u')M_3^3(s,u',u)\,,\\
\mathrm{dis}_sF_{NA}(s,u)&=\int du'F_3(s,u')M_{NA}^3(s,u',u)\,.
\end{aligned} \quad (4.10)$$

We seek a solution to (4.9) in the form

$$G_i(s)=F_C(s)d_i^C(s)+F_M(s)d_i^M(s)+\int duF_3(s,u)d_i^3(s,u)+\int duF_{NA}(s,u)d_i^{NA}(s,u)\,. \quad (4.11)$$

The absorptive parts of the d's can be obtained through an application of Eq. (4.6), and the d's from (4.7).

$$\begin{aligned}
d_i^{C,M}(s)&=\frac{1}{\pi}\int ds'\frac{A_i^{C,M}(s')}{s'-s}\,,\\
d_i^{NA}(s,u)&=\frac{1}{\pi}\int \frac{ds'}{s'-s}M_i^{NA}(s',u)\,,\\
d_i^3(s,u)&=\frac{1}{\pi}\int \frac{ds'}{s'-s}M_i^3(s',u)\\
&\quad-\frac{1}{\pi}\int \frac{ds'}{s'-s}\Big\{M_C^3(s',u)d_i^C(s')\\
&\quad+M_M^3(s',u)d_i^M(s')\\
&\quad+\int du'M_3^3(s',u,u')d_i^3(s',u')\\
&\quad+\int du'M_{NA}^3(s',u,u')d_i^{NA}(s',u')\Big\}\,.
\end{aligned} \quad (4.12)$$

Note that the d function for the three-pion state is given by an integral equation which involves all of the other d functions as inhomogeneous parts. The other d functions are determined directly from the contributions which appear in the unitarity statement. If one neglects the explicit three-pion contribution $F_3d_i^3$, then the result is just as if the nucleon form factors were to be factored out of the unitarity statement. Hence, this argument provides an explanation of the procedure employed in the previous section.

It seems worth-while to make two remarks about Eqs. (4.11) and (4.12). The first is the rather trivial point that these equations can be used to provide a simple distinction between additive and nonadditive parts of the form factor. The second is the more significant fact that by omitting the three-pion state in this way, we are in fact omitting only a part of the contribution from the three-pion diagram. This fact may explain why it is a good approximation to neglect the three-pion state when calculating the deuteron form factor, but not when calculating the nucleon form factor. The point is that when calculating the form factor in this way we may have already included the principal contribution from the three-pion diagram; another way to say this is that the inhomogeneous part of Eq. (4.12) for the deuteron is probably small, whereas the term involving M_i^3 (all that would occur in the analogous-nucleon problem) is almost certainly not small.

In practice one can calculate d_i^C and d_i^M quite accurately from the diagrams discussed in Fig. 5. Then, an estimate of the three-pion contribution can be made by choosing a set of phenomenological scattering amplitudes M^3 which satisfy coupled unitarity, and which are "calibrated" so that they yield correct nucleon form factors and phenomenological resonances.

ACKNOWLEDGMENTS

It is a pleasure to thank Professor M. L. Goldberger for his continuing guidance and Professor R. Blankenbecler for many invaluable discussions. Talks with Professor L. F. Cook, Jr., and Professor S. B. Treiman were helpful. I have also benefited from many informal talks with friends at Princeton and Cornell. My wife deserves special thanks for help with early stages of the manuscript.

APPENDIX

In this Appendix we first prove the following theorem, which is sufficient for our applications in Sec. 3:

Theorem: Let $f(s)$ and $g(s)$ be any rational functions with no poles such that $1/[f(s)-[g(s)]^{1/2}z]$ approaches zero at infinity for a dense set of z in $|z|\leqslant 1$. Then

$$I(s)=\int_{-1}^{+1}\frac{dz}{f(s)-[g(s)]^{1/2}z}=\int_C\frac{-ds'\,\mathrm{sgn}(p'(s'))}{[g(s')]^{1/2}(s'-s-i\epsilon)},$$

where $p(s)=f(s)/[g(s)]^{1/2}$ and the contour C is determined by

$$C:\quad s=p^{-1}(\alpha)\quad -1\leqslant\alpha\leqslant 1,$$

with the sense of integration in the direction of increasing s. The integration limits are at $s_0=p^{-1}(\pm 1)$.

Proof: We shall prove this by showing that both expressions have the same cuts in s. Then, they can differ only by an entire function, but since both approach zero at infinity this entire function can only be zero.

To show that they have the same cuts, consider

$$2i\,\mathrm{dis}_sI(s)=I(s^+)-I(s^-)=\int_{-1}^{+1}\frac{dz}{f(s^+)-[g(s^+)]^{1/2}z}-\int_{-1}^{+1}\frac{dz}{f(s^-)-[g(s^-)]^{1/2}z}.$$

Consider $s=s_0$ not a pole of f. Then f is real. Suppose g is negative. Then $g^{1/2}$ is pure imaginary and

$$2i\,\mathrm{dis}_sI(s)=\int_{-1}^{+1}\frac{dz}{f(s_0)-[g(s_0^+)]^{1/2}z}-\int_{-1}^{+1}\frac{dz}{f(s_0)+[g(s_0^+)]^{1/2}z}.$$

Because the denominator is never zero, we may transform $z\longrightarrow -z$ and

$$\mathrm{dis}_sI(s)=0.$$

Now consider the case when g is positive and $|f(s_0)|\geqslant|[g(s_0)]^{1/2}|$. Since $|z|\leqslant 1$, the denominators are never zero and again we may apply the same argument, obtaining zero for the discontinuity. Since the poles of f are discrete, they contribute discrete zeros to I and cannot influence the cut structure.

Finally, consider the case when $|f(s_0)|\leqslant|[g(s_0)]^{1/2}|$, g positive. In this case the denominators vanish, and we must take some care with the discussion. Introduce $p(s)=f(s)/[g(s)]^{1/2}$ and write

$$2i\,\mathrm{dis}_sI(s_0)=\int_{-1}^{+1}\frac{dz}{[g(s_0)]^{1/2}}\left\{\frac{1}{p(s_0^+)-z}-\frac{1}{p(s_0^-)-z}\right\}.$$

Note that

$$p(s_0^+)=p(s_0)+i\epsilon\,\mathrm{sgn}p'(s_0),$$
$$p(s_0^-)=p(s_0)-i\epsilon\,\mathrm{sgn}p'(s_0),$$

where

$$\mathrm{sgn}(x)=\begin{cases}+1 & x>0\\ -1 & x<0.\end{cases}$$

The $i\epsilon$ prescription tells us how to deform the contour so that the integral remains well defined. Hence, by Cauchy's theorem, we obtain

$$2i\,\mathrm{dis}_sI(s)=-2\pi i/[g(s_0)]^{1/2}\,\mathrm{sgn}p'(s_0).$$

The contour in the s plane along which this occurs is determined by

$$p(s)=\alpha,\quad s=p^{-1}(\alpha),\quad -1\leqslant\alpha\leqslant 1.$$

That the second expression for I has this discontinuity follows from the usual identity

$$\frac{1}{x'-x-i\epsilon}\longrightarrow\frac{\mathrm{P.V.}}{x'-x}+i\pi\delta(x'-x).$$

Hence the theorem is proved.

Corollary: Let $u(z)-m^2=f(s)-[g(s)]^{1/2}z$, where f and g have the properties described above. Suppose $h(x,u(z))$ is a real analytic function of u—i.e., $h^*(x,u)=h(x,u^*)$ for a certain range of x—and suppose that

$$\frac{h(x,u)}{u-m^2}\longrightarrow 0$$

as $s\longrightarrow\infty$ for a dense set of z in $|z|\leqslant 1$. Then

$$\int_{-1}^{+1}\frac{h(x,u)}{u-m^2}dz=\int_c\frac{h(x,m^2)\,\mathrm{sgn}(-p'(s'))ds'}{[g(s')]^{1/2}(s'-s-i\epsilon)}$$

for the same range of x. The contour C is as given above.

Proof: Since $u(z)=u^*(-z)$ when g is negative, the arguments above can still be applied. When g is positive, then u is real and hence h is real, and again the same arguments are valid. Finally, when the residue at the pole is calculated, u is set equal to m^2.

Remarks on Analytic Continuation

In this paper we have to continue some functions of the form

$$J(s,M^2)=\int_n^N \frac{ds'g(s')}{s'-s}\int_A^{a(M^2)}\frac{ds''f(s'')}{s''-s'},$$

where for small M^2, $a<n$, and of course $N>n$, $a>A$. The continuation is to be done in M^2. Characteristically, the upper limit, $a(M^2)$, migrates as a function of M^2. It is characterized in the cases of interest to us by

$$da/dM^2>0,\quad M^2<M_0^2,$$
$$a(M_0^2-i\epsilon)=n+\delta,\quad \delta>0,$$
$$da/dM^2<0,\quad M^2>M_0^2.$$

This is illustrated in Fig. 12. The upper limit of the s'' integral loops around the lower limit of the s' integral, forcing us to deform the s' contour if we wish to remain on the same (physical) sheet.[28]

The continuation can be done by giving M^2 a negative imaginary part. If M_f^2 is the final physical value of M^2, then the integral J becomes

$$J(s,M_f^2)=\left(\int_{a(M_f^2)+i\eta}^{n+i\eta}+\int_{n-i\eta}^{a(M_f^2)-i\eta}\right)\frac{ds'g(s')}{s'-s}\times\int_n^{a(M_f^2)}\frac{ds''f_c(s'')}{s''-s'}+\int_n^N\frac{ds'g(s')}{s'-s}\times\left\{\int_A^{a(M_f^2)}\frac{ds''f(s'')}{s''-s'}+\int_{a(M_f^2)}^n\frac{ds''}{s''-s'}[f(s'')-f_c(s'')]\right\},$$

where f_c is the continuation of f in s'' around the point n. In general f may have a cut starting at n, and hence f_c will not be the same as f. Using Cauchy's theorem and letting $a=a(M_f^2)$, $\eta\to 0$ we have

$$J(s,M_f^2)=-\int_a^n\frac{2\pi i ds''f_c(s'')g(s'')}{s''-s}+\int_n^N\frac{ds'g(s')B(s')}{s'-s},$$

where

$$B(s')=\int_A^a\frac{ds''f(s'')}{s''-s'}+\int_a^n\frac{ds''}{s''-s'}[f(s'')-f_c(s'')].$$

In general, in our applications we shall retain only the first integral, which is the integral over the anomalous region.

Note that the factor $(s'-s)^{-1}$ played no role in the argument, so we would obtain similar results without it.

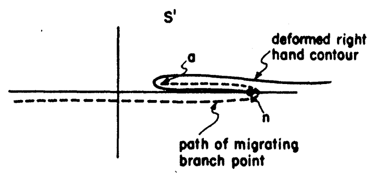

FIG. 12. Deformation of the right-hand contour in the complex s' plane necessitated by the migrating branch point of the integrand.

[28] R. Blankenbecler, M. L. Goldberger, S. W. MacDowell, and S. B. Treiman, Phys. Rev. 123, 692 (1961).